

Statistical Equilibria of Uniformly Forced Advection Condensation

Jai Sukhatme¹ and Raymond T. Pierrehumbert²

¹ National Center for Atmospheric Research, Boulder, CO 80305

² Department of Geophysical Sciences, University of Chicago, Chicago, IL 60637

(Dated: May 24, 2019)

We examine the state of statistical equilibrium attained by a uniformly forced condensable substance subjected to advection in a periodic domain. In particular, working in limit of rapid condensation we study the probability density function (PDF) of the condensable field whenever the advecting velocity field admits a diffusive representation in the Boltzmann equation governing evolution of probability. Following a peak at small values of the condensable field, the derived PDF decays exponentially before terminating in an abrupt "roll-off" due to the constraint imposed by rapid condensation. A set of simple numerical exercises are performed to test these features. Also, despite the simplifications involved, the derived PDF compares favourably with atmospheric water vapor data.

PACS numbers: PACS number 47.52.+j, 05.45.-a

I. INTRODUCTION

Advection-Diffusion-Condensation (ADC) is a variant of the familiar passive advection-diffusion problem [1], wherein apart from molecular diffusion a tracer is subject to an additional sink associated with the process of condensation. A study of the interplay of these processes is motivated by the need to understand the large scale distribution of water vapor in the troposphere [2],[3],[4]. Indeed, the prominent role played by water vapor in various problems related the Earth's climate [5] — for example, via the water vapor feedback in the greenhouse effect [6] — makes this an important issue. In this context, ADC serves as an idealized problem for water vapor in the troposphere [7]. The mixing ratio $q(\vec{x}, t)$ of a scalar tracer subject to advection, diffusion and condensation is governed by

$$\frac{\partial q}{\partial t} + (\vec{u} \cdot \nabla)q = \eta \nabla^2 q + S(q, q_s) + F \quad (1)$$

here \vec{u} and F are the advecting velocity field and the forcing respectively and η is the diffusivity of the condensable substance. In the present work we shall assume the domain to be spatially bi-periodic and restrict our attention to the nondiffusive limit, $\eta = 0$. The problem thus consists of the advection of a passive tracer supplied by the source F , and removed by a sink associated with condensation. This sink is represented as

$$\begin{aligned} S &= -\frac{1}{\tau}[q - q_s(\vec{x})] & \text{if } q > q_s \\ &= 0 & \text{if } q \leq q_s \end{aligned} \quad (2)$$

where $q_s(\vec{x})$ is the saturation mixing ratio — a prescribed function. In a sense, the ADC problem bears a similarity recent studies of "active" processes when coupled with fluid advection, such as the evolution of chemically [8] or biologically [9] active substances and the issue of phase separation in immiscible fluids [10].

Our aim is to examine the state of statistical equilibrium attained by (1) and (2) in the limit $\tau \rightarrow 0$ or that of *rapid condensation*. This limit implies that upon advection if $q(\vec{x}, t) > q_s(\vec{x})$, then the parcel's mixing ratio is instantaneously reset to the saturation mixing ratio at that location. Of course, two immediately apparent opposing long time limits of (1) and (2) are : (i) Uniform forcing with $u = 0 \Rightarrow q(\vec{x}, t) \rightarrow q_s(\vec{x})$ and (ii) A sufficiently mixing flow with $F = 0 \Rightarrow q(\vec{x}, t) \rightarrow \min_{\forall \vec{x}}[q_s(\vec{x})]$. Hence, to achieve a non-trivial state of statistical equilibrium we require both $\vec{u}, F \neq 0$.

In the absence of diabatic effects, parcel motion in the midlatitude troposphere is restricted to two-dimensional surfaces of constant potential temperature, i.e. to isentropic surfaces [11]. Our objective is to understand the probability density function (PDF) of the water vapor mixing ratio along these midlatitude isentropic surfaces [12]. On average the thermal structure of the midlatitude troposphere is such that as one progresses polewards, the temperature along

isentropic surfaces decreases in a fairly linear manner. Given the sensitivity of the saturation mixing ratio (via the Clausius-Clapeyron relation) to the temperature, following [7] we take q_s to vary exponentially with y . As we are in a periodic domain, $q_s(\vec{x}) = q_s(y) = \exp(-\alpha|y - \frac{L}{2}|)$ ($0 \leq y \leq L$) where $\alpha > 0$ and increasing α yields progressively steeper profiles which fall off symmetrically from $y = \frac{L}{2}$. This yields an idealized model problem which retains the essence of the much more complex atmospheric problem that motivates our work. Even though the real atmosphere does not conform exactly to the idealizations, progress can be made through a detailed solution of this model problem.

II. THE PDF IN THE LIMIT OF RAPID CONDENSATION

The Liouville or transport equation satisfied by the PDF for a single realization of (1) with $\eta = 0$ is

$$\frac{\partial P(x, y, q, t)}{\partial t} + \frac{\partial(u_i P)}{\partial x_i} + \frac{\partial[(F + S)P]}{\partial q} = 0 \quad (3)$$

but in the limit of rapid condensation, we have $0 \leq q(x, y, t) \leq q_s(y)$. Hence (3) becomes

$$\frac{\partial P(x, y, q, t)}{\partial t} + \frac{\partial(u_i P)}{\partial x_i} + \frac{\partial(FP)}{\partial q} = 0$$

with $P(x, y, q, t) = 0$ for $q(x, y, t) > q_s(y)$ (4)

As the saturation mixing ratio is purely a function of y , if the forcing is also taken to be of the form $F = F(y)$ (in fact we will focus on the uniformly forced case) — it is reasonable to look for stationary solutions of (4) which are independent of x , i.e. $P = P(q, y)$. Of course, it is the realization of statistical equilibrium without the presence of gradient fields (as $\eta = 0$) that makes progress possible in the present case [21]. This circumvents the need to estimate conditional expectations of the scalar dissipation (or diffusion) which complicate advection-diffusion problems [14], [15], [16].

We now assume that the effect of the fluctuating velocity in the Liouville equation admits a diffusive representation — say by an eddy diffusivity κ_e . This would be the case if the parcel trajectories consisted of independent Brownian motion, for example. Admittedly, this is a fairly severe assumption in that mixing by multiple scale velocity fields rarely follows a simple diffusive prescription [17]. But from a tropospheric viewpoint, it is known that the meridional (y - direction) Lagrangian eddy-velocity correlation function decays quite rapidly (on the order of a few days) [18] — hence, in this context the assumption of an eddy diffusivity may not completely unreasonable. Note that the eddy diffusivity we refer to here is an eddy diffusivity applied to probability evolution in (y, q, t) space. This is not the same as characterizing mixing by an eddy diffusivity to an evolution equation for a coarse-grained q in (y, t) space. Indeed, in [7] it is shown that the Brownian model yields different coarse-grained q statistics than the mean-field diffusivity model; it is suggested further that the Brownian motion model constitutes a minimal model for investigation of the interplay of transport processes with a nonlinear sink term such as condensation. In that sense, the Brownian model is worth of study in and of itself.

For the Brownian representation (4) becomes

$$-\kappa_e \frac{\partial^2 P}{\partial y^2} + F(y) \frac{\partial P}{\partial q} = 0 \quad (5)$$

Substituting a separable form, i.e. $P(y, q) = A(q) B(y)$ in (5) gives

$$\begin{aligned} \frac{d \log(A(q))}{dq} &= \pm k^2 \\ \frac{d^2 B}{dy^2} &= \pm \frac{k^2}{\kappa_e} F(y) B(y) \end{aligned} \quad (6)$$

For uniform forcing, i.e. $F(y) = \delta$ (a constant) we choose the separation constant to be $-k^2$ as $P(q, y)$ is periodic in y .

$$P(q, y) = \sum_{m=1}^{\infty} \exp(-k^2 q) [C_m \cos(\lambda y) + D_m \sin(\lambda y)]; \quad \lambda = \frac{m\pi}{L} \quad (7)$$

which fixes $k^2 = \lambda^2 \frac{\kappa_e}{\delta}$ and in effect after choosing L the only free parameter is the ratio $\frac{\kappa_e}{\delta}$.

To obtain PDF of q we estimate the probability that $q < Q$ as a function of Q (i.e. Q represents the sample space variable corresponding to q). As $P(q, y) = 0$ for $q(x, y, t) > q_s(y)$, $P(q, y)$ has to be integrated with respect to the saturation curve $q_s(y)$. Therefore,

$$Pr(q < Q) = \frac{I_1 + I_2}{I_t} \quad (8)$$

Here I_1, I_2 correspond to the regions $y \leq Y$ and $y > Y$ where $Y = F(Q)$ (F being the inverse of $q_s(y)$). Specifically,

$$\begin{aligned} I_1 &= \int_0^{F(Q)} \int_{Q_2}^Q P(q, y) \, dq dy \\ I_2 &= \int_{F(Q)}^L \int_{Q_2}^{q_s(y)} P(q, y) \, dq dy \end{aligned} \quad (9)$$

where $Q_2 = \min(q_s)$. I_t in (8) is the same as I_2 but with 0 as the lower limit of integration in the outer integral. Substituting for $P(q, y)$ and setting $dG_m/dy = [C_m \cos(\lambda y) + D_m \sin(\lambda y)]$ for notational simplicity,

$$I_1(m) = \frac{[-\exp(-k^2 Q) + \exp(-k^2 Q_2)]}{k^2} [G_m(F(Q)) - G_m(0)] \quad (10)$$

Similarly,

$$I_2(m) = \frac{\exp(-k^2 Q_2)}{k^2} [G_m(L) - G_m(F(Q))] - \frac{X(m)}{k^2} \quad (11)$$

where

$$X(m) = \int_{F(Q)}^L \frac{dG_m(y)}{dy} \exp[-k^2 q_s(y)] \, dy \quad (12)$$

As I_t is independent of Q it only affects the normalization of the PDF. Hence,

$$\text{PDF}(Q) \sim \frac{d(I_1 + I_2)}{dQ} = \sum_{m=1}^{\infty} \exp(-k^2 Q) [G_m(F(Q)) - G_m(0)] \quad (13)$$

Substituting for $G_m(y)$

$$\text{PDF}(Q)_m \sim \frac{\exp(-k^2 Q)}{\lambda} \{C_m \sin[\lambda F(Q)] - D_m \cos[\lambda F(Q)] + D_m\} \quad (14)$$

Substituting for $F(Q)$ (as q_s is symmetric about $y = \frac{L}{2}$ we need only consider half of the domain with $q_s = \exp(-\alpha y)$, i.e. $F(Q) = -\log(Q)/\alpha$) with $C_m, D_m = 1 \forall m$

$$\text{PDF}(Q) \sim \sum_{m=1}^{\infty} \frac{\exp(-k^2 Q)}{\lambda} \{\sin[\log(Q^{\frac{-\lambda}{\alpha}})] - \cos[\log(Q^{\frac{-\lambda}{\alpha}})] + 1\} \quad (15)$$

The dependence of the PDF on $\frac{\kappa_e}{\delta}$ and α is shown in the upper and lower panels of Fig. (1) respectively. In all cases the PDF has a peak for small q , decreases exponentially for intermediate values of q and then "rolls-off" very rapidly at high q . It is the rapid condensation constraint, i.e. $q(x, y, t) \leq q_s(y)$ that is responsible for this "roll-off" when $q \approx \max_{\forall y} [q_s(y)]$.

Further, even though the principal structure of the condensable field is controlled by the saturation mixing ratio profile, the PDF in (14) is in marked contrast to what one would obtain for a fully saturated domain. For example in the saturated case, assuming a uniform distribution of particles in y immediately gives $\text{PDF}(Q_{\text{sat}}) \sim -dF(Q)/dQ$ which leads to a power law (Q^{-1} , with no "roll-off" for high Q) when $q_s = \exp(-\alpha y)$.

III. NUMERICAL SIMULATIONS

A primary assumption in our derivation was the use of an "eddy diffusivity" to represent the effect of an advecting velocity field on the evolution of probability. As mentioned, in most flows of interest the velocity field is expected to be quite coherent and might not conform to a diffusive representation. To test the stringency of this assumption we numerically simulate the ADC system by employing a lattice map for purposes of smooth large scale advective mixing [19],[20]. The velocity field is

$$\begin{aligned} u(x, y, t) &= f(t) A_1 \sin(y + p_n) \\ v(x, y, t) &= (1 - f(t)) A_2 \sin(x + q_n) \end{aligned} \tag{16}$$

where $f(t)$ is 1 for $nT \leq t < (n+1)T/2$ and 0 for $(n+1)T/2 \leq t < (n+1)T$. p_n, q_n ($\in [0, 2\pi]$) are random numbers selected at the beginning of each iteration, i.e., for each period T . Advection is implemented via sequential integer shifts in the x and y directions respectively (see [19] for details). Apart from its numerical efficiency the lattice map has the advantage of preserving moments, i.e. it does not introduce spurious diffusion into the problem. Opposing initial conditions, a completely dry and a fully saturated domain, are used to start the simulations with a uniform forcing applied at every iteration. Fig. (2) shows the ratio of the total substance being condensed out at every step to the forcing and the spatial average of the condensable field as a function of the iteration. As is seen both initial conditions settle into the same state of equilibrium.

To test our theoretical estimate of the PDF of q we vary α for a fixed forcing strength (i.e. fixed $\frac{\kappa_e}{\delta}$). The PDF's after equilibrium is achieved are shown in Fig. (3) — the plotted PDF's are averages over the last couple of iterations of the map. In spite of the non-local nature of the mixing protocol the shapes of the PDF's follow theoretical estimates derived under a eddy-diffusive approximation [22]. The disagreement between the numerical and theoretical PDF's is expected for small q as $\delta > \min_{\forall \vec{x}} [q_s(\vec{x})]$ and therefore for $q < \delta$, the numerical PDF actually represents saturation [23].

Of course, as is evident from (15) for a fixed flow (i.e. fixed κ_e) the mean of the condensable field is a function of the forcing strength. In fact, as is seen in Fig. (4) — which shows the numerically computed mean as well as the mean using the first mode of (15) — the mean of the condensable field increases with the forcing strength until $\delta = \max_{\forall \vec{x}} [q_s(\vec{x})]$ when the entire domain becomes saturated.

IV. CONCLUSIONS AND ATMOSPHERIC DATA

We have examined the state of equilibrium achieved via the interplay of smooth advection and condensation. Exploiting the attainment of equilibrium without the presence of gradient fields allows us to make progress on the Liouville equation governing the PDF of the condensable substance. The analytically estimated PDF, derived in the limit of *rapid condensation* with the assumption of an eddy-diffusivity, is seen to compare favourably with numerical simulations. Even though in the present situation we are dealing with the case $\eta = 0$, the presence of a slowly decaying PDF is not entirely unexpected when taken in the context of passive advection-diffusion studies [1]. It is

the rapid "roll-off" for $q \approx \max_{\vec{x}}[q_s(\vec{x})]$ that stands out as a characteristic feature of the PDF.

As mentioned in the Introduction, our motivation is to understand the distribution of water vapor along midlatitude isentropic surfaces. With this in mind we construct PDF's of the midlatitudinal specific humidity field along the 300 K isentrope using data from the ECMWF reanalysis (ERA40) project. As is seen in Fig. (5), despite the simplifying assumptions made in our derivation, the PDF's from data bear a fair resemblance to theory. It is for large q that the PDF's from data deviate significantly from the theoretical estimate. As we have considered the nondiffusive limit a possible source of this discrepancy might lie in the homogenization induced by diffusion. Secondly, as the source of water vapor lies in the tropics a boundary forcing might be more appropriate for the actual atmospheric problem. Even so, these moderately encouraging results lead us to conjecture that the ADC model driven by idealized velocity fields might be of use in predicting the statistical properties of the large scale distribution of water vapor in the midlatitude troposphere. Indeed, this is the focus of ongoing work.

Acknowledgments

We are very grateful to Prof. W.R. Young (Scripps Institute, UCSD) for his suggestions and insight which led to a clear formulation of the problem. J.S. would also like to acknowledge numerous conversations with Dr. A. Alexakis (NCAR). This work was carried out while the first author was at the National Center for Atmospheric Research which is sponsored by the National Science Foundation. The second author's contribution to this work was sponsored by the National Science Foundation under grant ATM-0123999.

[1] G. Falkovich, K. Gawedzki and M. Vergassola, Rev. Mod. Physics, **73**, 913 (2001).
[2] S.C. Sherwood, J. Climate, **9**, 2919 (1996).
[3] E.P. Salathe and D.L. Hartmann, J. Climate, **10**, 2533 (1997).
[4] R.T. Pierrehumbert, Geophys. Res. Lett. **25**(2), 151 (1998).
[5] R.T. Pierrehumbert, Nature, **419**, 191 (2002).
[6] I. Held and B. Soden, Annu. Rev. Energy Environ. **25**, 441 (2000).
[7] R.T. Pierrehumbert, H. Brogniez and R. Roca; in *The General Circulation of the Atmosphere*, edited by T. Schneider and A. Sobel (Princeton University Press, 2005) (to appear).
[8] Z. Neufeld, C. Lopez and P.H. Haynes, Phys. Rev. Lett. **82**, 2606 (1999).
[9] E.R. Abraham, Nature, **391**, 577 (1998).
[10] L. Berthier, J-L. Barrat and J. Kurchan, Phys. Rev. Lett. **86**, 2014 (2001).
[11] B. Hoskins, Tellus, **43AB**, 27 (1991).
[12] H. Yang and R.T. Pierrehumbert, J. Atmos. Sci. **51**, 3437 (1994).
[13] M. Chertkov, Phys. of Fluids, **10**(11), 3017 (1998).
[14] S.B. Pope, Prog. Energy Combust. Sci. **11**, 119 (1985).
[15] C. Dopazo, L. Valino and N. Fueyo, Int. Journal of Mod. Physics B, **11**, 2975 (1997);
[16] J. Sukhatme, Phys. Rev. E, **69**, 056302 (2004).
[17] A.J. Majda and P.R. Kramer, Physics Reports, **314**, 238 (1999).
[18] J. Sukhatme, J. Atmos. Sci. **62**, 3831 (2005).
[19] R.T. Pierrehumbert, Chaos, **10**, 1, 61 (2000).
[20] J. Sukhatme and R.T. Pierrehumbert, Phys. Rev. E, **66**, 056302 (2002).
[21] A similar absence of gradient fields in equilibrium has been indirectly exploited in the study of advection with linear damping [13].
[22] Here $\delta = 0.05$. Hence, assuming $\kappa_e \sim 1 \Rightarrow \frac{\kappa_e}{\delta} \approx 20$.
[23] When $\frac{\kappa_e}{\delta}$ is increased for a fixed α we observe (not shown) the slope of the PDF to become steeper in accordance with Fig. (1).

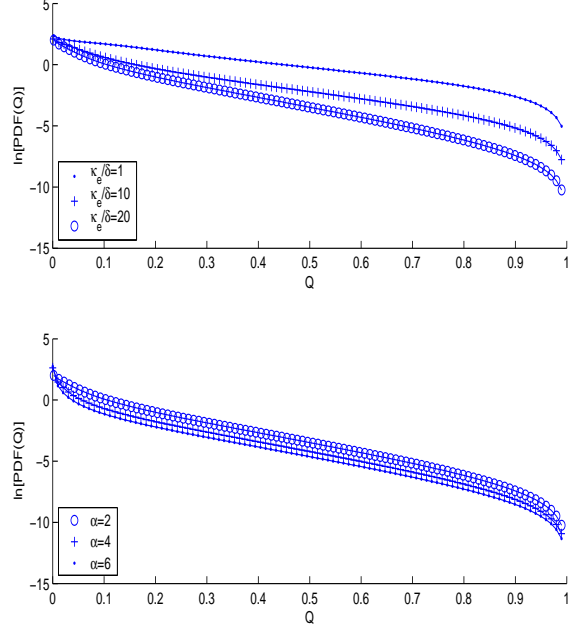


FIG. 1: The PDF in (15) with $L = 2\pi$. Upper panel : Varying $\frac{\kappa_e}{\delta}$ with $\alpha = 2$. Lower Panel : Varying α with $\frac{\kappa_e}{\delta} = 20$.

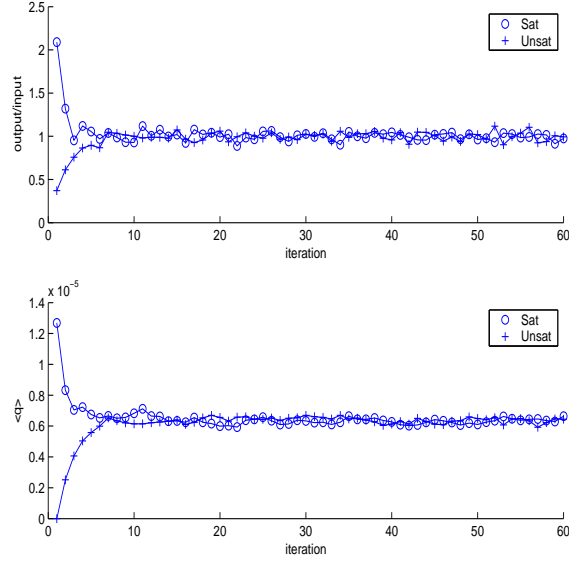


FIG. 2: Upper Panel : The total amount that condenses out of the domain divided by the total input into the domain as a function of iteration. As expected this $\rightarrow 1$, i.e. we achieve a balance between the forcing and the sink, as we settle into equilibrium. Lower Panel : Spatial average of q .

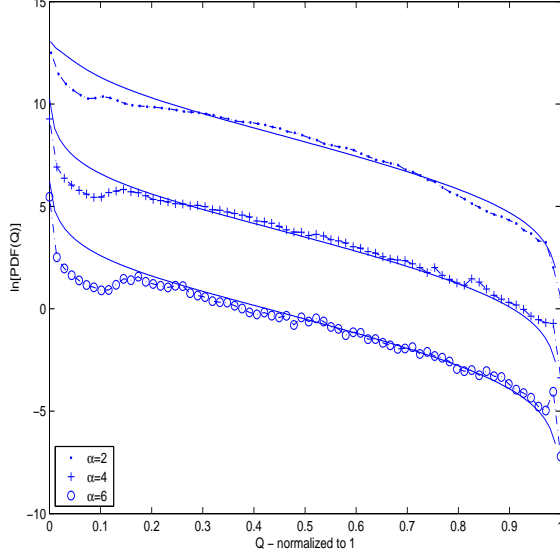


FIG. 3: The PDF using the lattice map for $\alpha = 2, 4, 6$ with constant forcing ($\delta = 0.05$). The curves have been shifted for clarity. The solid lines are plots of (15) (shifted vertically by a constant) with $\frac{\kappa_e}{\delta} \approx 20$.

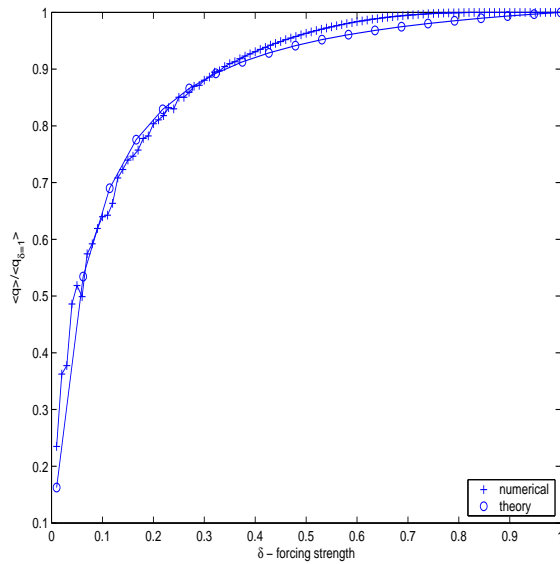


FIG. 4: The effect of varying the forcing strength on $\langle q \rangle$ both numerically and using a single mode of (i.e. $m = 1$) (15) ($L = \pi, \kappa_e = 1$). The mean of the condensable field increases with δ until $\delta = \max_{\vec{x}}[q_s(\vec{x})]$ where the domain becomes fully saturated.

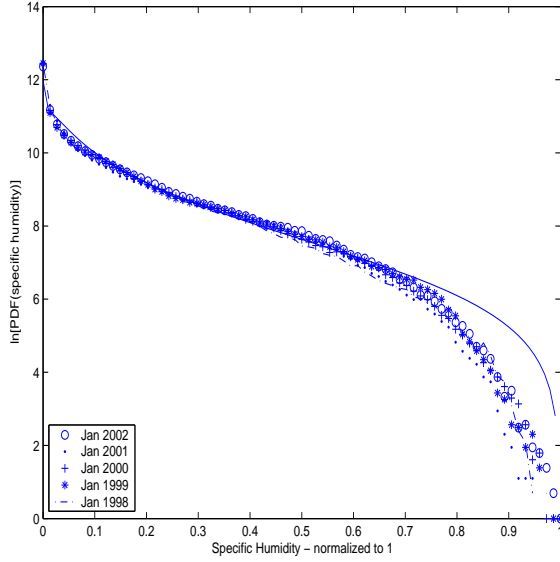


FIG. 5: The normalized specific humidity PDF's in the midlatitudes (between 30° and 60° in both hemispheres) along the 300 K isentropic surface for Jan 97-02 from ECMWF data. The solid line is a plot of (15) with $\frac{\kappa_e}{\delta} = 2.5$, $\alpha = 4$, $L = 2\pi$